Microstructural and mechanical properties of double-sided MIG, TIG and friction stir welded 5083-H321 aluminium alloy

E. Taban[1], E. Kaluc[2]*

[1] *Department of Mechanical Engineering, Engineering Faculty, Kocaeli University, Kocaeli 41040, Turkey*
[2] *Welding Technology Research and Training Center, Veziroglu Campus, Kocaeli University, Kocaeli, 41040, Turkey*

Received 26 May 2005, accepted 14 December 2005

Abstract

In this study, strain-hardened EN AW-5083-H321 aluminium alloy plates were welded using MIG, TIG and friction stir welding (FSW) processes in order to investigate microstructural and mechanical properties, respectively. As a microstructural investigation, light microscopy and image analysis system were used for double-sided MIG, TIG and FSW specimens weld zones. Measurements of hardness were carried out using the microhardness tester with 200 g test load on metallografic specimens taken from each welded plate. Tensile and bend tests were applied to specimens taken from welded plate with reference to EN 895 and EN 910 standards. Fracture surfaces were also examined using light microscopy and scanning electron microscopy. As a result, it has been observed that FS welded joints have relatively superior properties as/than MIG and TIG welded joints.

K e y w o r d s: 5083-H321, MIG, TIG, friction stir welding (FSW), microstructural and mechanical properties

1. Introduction

Aluminium and aluminium alloys are common structural materials due to their attractive combination of properties including light weight, moderate strength, good corrosion resistance, workability, proven weldability and good electrical and thermal conductivity. Hence these alloys are commonly used in automotive, railway, shipbuilding and defence industries, aviation and aerospace industries [1–5].

For the joining of aluminium alloys, besides fusion welding processes, solid state welding processes have been widely being used in various industrial applications. There are, however, a number of mechanical and metallurgical problems associated with the fusion welding of aluminium and its alloys such as decreasing strength and metallurgical precipitations in the weld metal and heat affected zone (HAZ), distortions, residual stresses due to high heat input, gas porosity, lack of fusion, high coefficient of thermal expansion, solidification shrinkage, high solubility of hydrogen and other gases. The joining of aluminium alloys, especially those which are often difficult to weld, has been the initial target for developing the new solid state welding – friction stir welding (FSW) [1, 6]. The FSW technique (invented, patented and developed by TWI) enables the advantages of solid phase welding to be applied to the fabrication of long butt and lap joints with very little post weld distortion. FSW operates by passing a rotating tool between two plates that are restricted from movement. The tool is plunged into the material to a preset depth and moved along the weld joint. Heat is generated through frictional contact between the rotating tool shoulder and abutting material surface. Despite being such relatively new process, friction stir welds have already been launched into aircraft, shipbuilding, automotive, railway, defence industries with great success and the process being actively investigated for further applications [1, 4–9].

While examining the literature on this subject, it has been found that a number of research studies have

*Corresponding author: tel.: +90 262 3351148 (ext. 1147); fax: +90 262 3352812; e-mail address: ekaluc@kou.edu.tr

Table 1. Chemical composition and mechanical properties of 5083-H321 aluminium alloy

Chemical composition [wt.%]										
Si	Fe	Cu	Mn	Mg	Cr	Ni	Zn	V	Ti	Al (min)
0.117	0.245	0.071	0.488	4.7	0.108	0.001	0.083	0.016	0.041	Rem.

Mechanical properties		
Proof strength $R_p0.2$ [MPa]	Tensile strength R_m [MPa]	Elongation (min) [%]
259	355	13.2

been done on the friction stir weldability of 5083 aluminium alloy [8, 10–18]. However, there has not been enough information reported concerning the comparison of the mechanical and microstructural properties of welded zones of double-sided MIG, TIG and FS welded 5083-H321 alloy.

The aim of the present paper is to determine and discuss microstructural observations and provide information about the mechanical properties of double-sided MIG, TIG and FS welded 5083-H321 aluminium joints. After mechanical tests, the fracture surfaces of weld zones have been examined using LOM and SEM and discussed.

2. Material and experimental procedure

The base material used in this study was 6.45 mm thick 5083-H321 aluminium alloy, which is a non-heat treatable Al-Mg alloy with relatively good mechanical properties and corrosion resistance commonly used in defence and shipbuilding industries. This alloy has a relatively large Mg content to promote solid solution strengthening and to increase the rate of work hardening, the most important strengthening mechanisms in this alloy. Manganese increases the recrystallisation temperature and improves the strengthening effect of magnesium [19]. Chemical composition and mechanical properties of the alloy are listed in Table 1.

5083-H321 aluminium alloy plates were cut into 6.45 × 150 × 350 mm coupons with a 30° level of each plate to provide 60° groove angle for a double V-groove (symmetric X-groove) butt joint configuration according to EN ISO 9692-3 for MIG and TIG welding. The root face was 1 mm with root opening of 2 mm. Only I-groove butt welding preparation was applied for FSW process without root opening.

MIG and TIG joints were realised semi-automatically in industrial conditions. Chemical oxide removal processes were applied prior to and before welding all grooves have been cleaned from all contaminations by using acetone and stainless steel brush. Detailed parameters are: voltage 24–26 V, welding current 180–200 A, 99.999 % Argon as shield gas (flow rate 12 l/min), 1.6 mm diameter ER 5356 (AlMg5Cr(A)) filler metal were used.

6.45 mm thick plates were friction stir welded using AISI 4340 (0.40 % C, 0.70 % Mn, 0.30 % Si, 0.80 % Cr, 1.80 % Ni, 0.25 % Mo) tool. Shoulder diameter was 20 mm and the pin was standard M5 threaded and 3.6 mm height. The tool rotational speed was set equal to 1600 rpm and translation speed was 125 mm/min. The tool was tilted at 2° from the plate normal and rotated in the anti-clock direction. The specimens were tightly fixed at the machine tool table. Before FSW, weld groove was cleaned with acetone and brushed by stainless steel brush carefully.

After welding, a visual inspection was made on all welded plates in accordance with ANSI/AWS B1.11. All weld defects were examined from both the front and back side of weld bead carefully. Weld reinforcement and spatter dimensions were also measured. All welded joints were subjected to distortion measurements. Angular displacements in butt joint welded plates were inspected.

MIG, TIG and friction stir welded joints were cross-sectioned perpendicular to the welding direction for metallographic analyses. The cross-sections of the metallographic specimens were polished with diamond suspension and colloidal chemical, etched with modified Keller's reagent (2 ml HF, 3 ml HCl, 20 ml HNO_3, 175 ml H_2O) at room temperature for about 30 s. They were visualised as macrographs and subsequently observed by light microscope. Metallography and hardness variations with 200 g test load were carried out on all as-welded samples in a section across the weld of the first and second pass, respectively. Future-Tech FM 700 Microhardness Tester having a loading capacity of 10 g minimum was used for the hardness measurements.

The tranverse tensile and bend test specimens were taken and prepared from MIG, TIG and FS welded plates with reference to EN 895 and EN 910 standards, respectively. Tensile and bend tests were carried out using servo-hydraulic controlled DARTEC test machine at room temperature. Weld reinforcement of the specimens was ground off.

After tensile test, fracture surfaces of broken samples were examined using light macro-stereomicro-

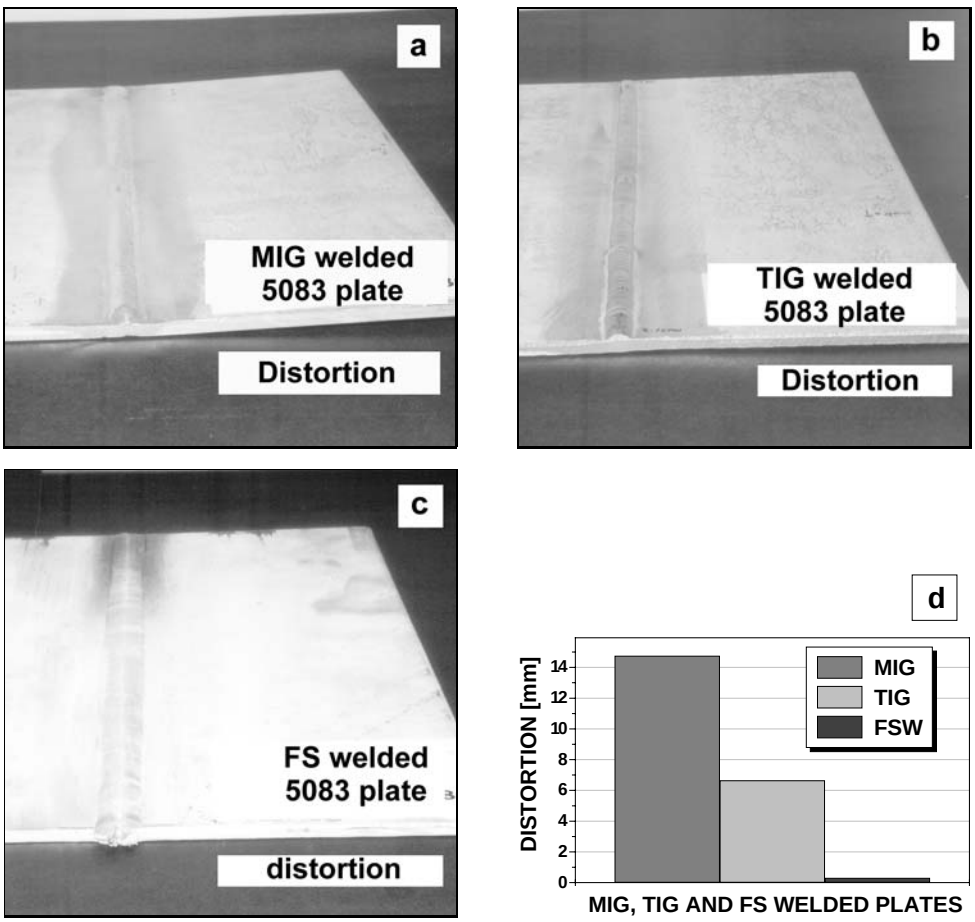

Fig. 1. Distortion phenomena of double-sided welded plates: the photographs for the distortion of MIG (a), TIG (b) and FS (c) welded plates, the graph showing the comparison of welded plates distortion rates (d).

scopy and SEM in order to determine the fracture mode of welded joints. Also, bend test samples were investigated using macro-microscopy in order to examine the surface cracks of face and root sides on weld beads.

3. Results and discussion

As a result of visual inspection on welded plates, it was observed that welds of both MIG and TIG welded joints were in acceptable limits; there was not too much spatter, the sizes of spatter were very small and no surface cracks and discontinuities were detected. The surface appearance of FS welded joints was a regular series of semi-circular ripples. No surface cracks and discontinuities were detected. Investigations have shown that the distortions in MIG and TIG welded plates were much higher than in FS welded joints nevertheless still they were within the acceptable limits. Double-sided MIG, TIG and FS welded plates were compared for dimensional accuracy using angular distortion measurements. FS welded plates exhibited much better dimensional accuracy mostly due to the fact, that the materials had not been melted during the welding process. It is known that the maximum temperature for aluminium FS welds is far lower than that of MIG and TIG welding. Increase in the temperature during welding results in greater distortion. The total distortion of 14.75 mm was measured for MIG welded plate, 6.65 mm for TIG welded and 0.5 mm for FS welded joints. The largest distortion amount was determined for MIG welded joints. Because the heat input of TIG welding is local, the distortion rate of the TIG plate was less than that of MIG welded plates. Figures 1a,b,c show the photos of distortion of as-welded plates and Fig. 1d shows the comparison of the amount of distortion for three welding methods.

The microstructural investigation was carried out on the metallographic specimens of the joints using light microscope with 50× and 200× magnifications. The investigation of the weld metal was performed with the order of base metal (BM)-heat affected zone (HAZ) for fusion welding processes and thermomechanically affected zone (TMAZ) for FSW- and weld

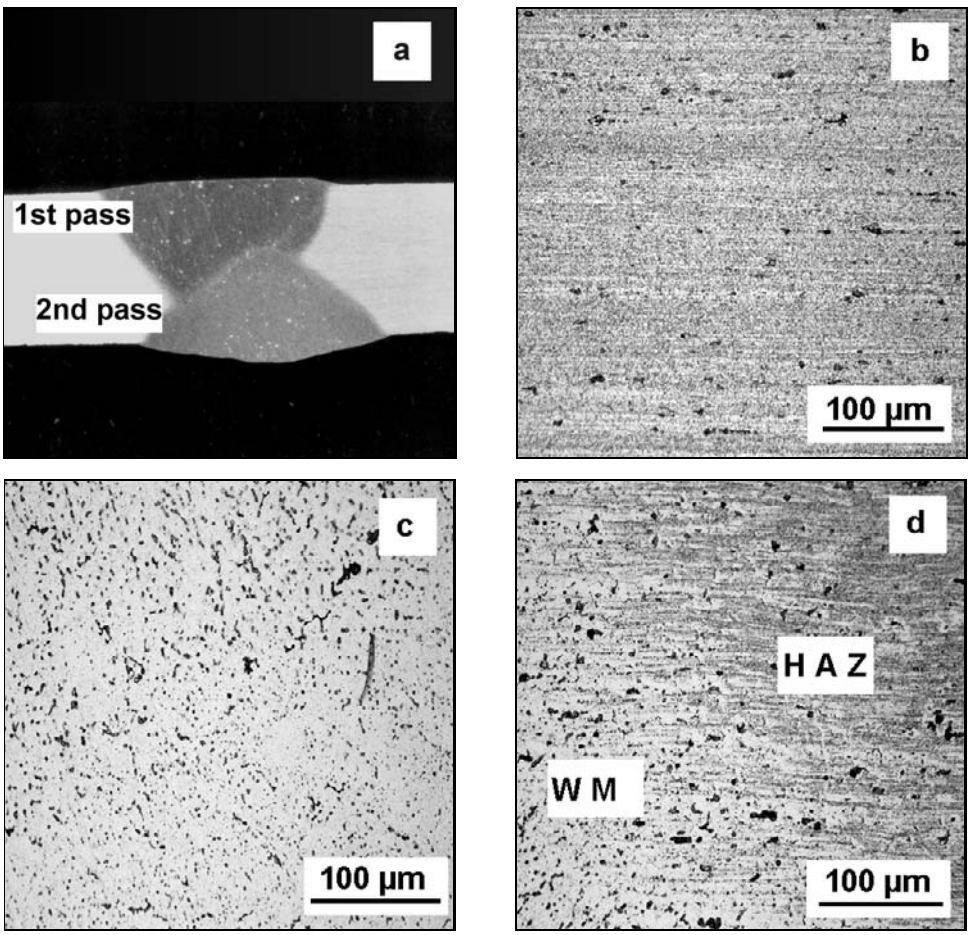

Fig. 2. Light macrostructure of MIG welded 5083-H321 alloy (a) and first pass microstructures of the alloy: BM (b), WM (c), HAZ + WM (d).

metal (WM). Figures 2 and 3 show the macrographs and micrographs of first passes of double-sided MIG and TIG welded zones, respectively; Figure 4 shows the macrograph and micrographs of both first and second passes of double-sided friction stir welded zones of 5083-H321 specimens.

It is known that, in case of fusion welding processes such as MIG and TIG welding, due to the fusion of material and high temperatures experienced by adjacent material relatively wide HAZ appears. The 5xxx series alloys are work hardenable alloys and so the base metal microstructure is observed as typical of rolling/work hardening microstructure. It was seen that MIG and TIG weld metals consist of dendrites with fine precipitates of Mg_2Al_3 (dark) as typically ER 5356 filler metal microstructure [20]. A number of microvoids and porosities were also observed in the weld metal of MIG welded samples (see Figs. 2a,c). These are the potential sources for cracks during the service conditions. Unlike the case of heat treatable alloys, whose strengthening precipitates may dissolve or coarsen, the HAZ damage in non-heat treatable alloys is limited to recovery, recrystallisation and grain growth. Thus, loss in strength in the HAZ is not nearly as severe as that experienced in heat treatable alloys. HAZ in fusion welded samples contains typical features [19]. Because of the same filler metal ER 5356 used for TIG welding, similar weld metal structure was observed, however no porosity was determined. Similar base metal and HAZ morphologies appeared as seen in Fig. 3.

The structure of FS welds contains features that are not found in fusion welds. The reason is that, unlike fusion welding processes, no filler metal was used and no groove preparation was used in FSW process. The structure of the weld zone, due to severe mechanical stresses experienced by the material, shows a variety of zones. A fine-grained structure is characterised by the presence of so-called onion rings, which appear across the section and allow a partial recovery of mechanical properties. This onion ring structure of the nugget is typical of high quality stir weld, in which neither porosity nor microvoids are detected. In the double-side welded friction stir welding of

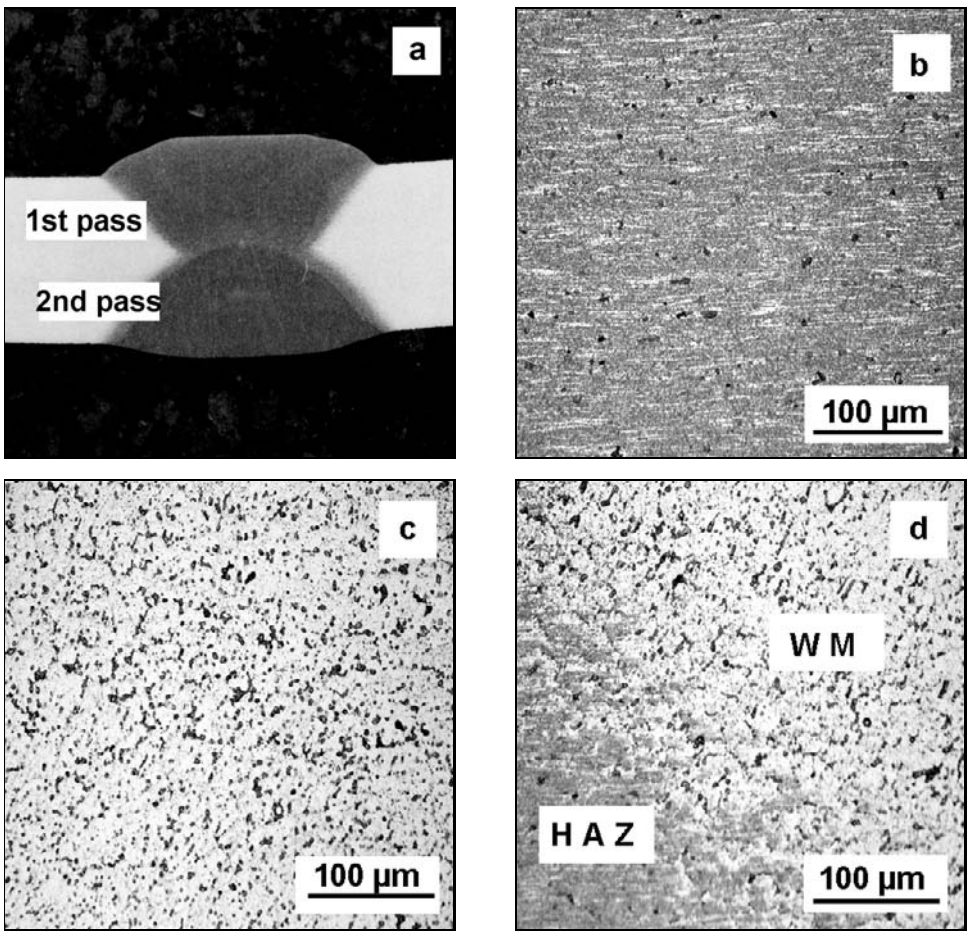

Fig. 3. Light macrostructure of TIG welded 5083-H321 alloy (a) and first pass microstructures of the alloy: BM (b), WM (c), WM + HAZ (d).

this alloy, two nugget zones were clearly observed in macro-section of the joints as seen in Fig. 4a. Figure 4b shows the base metal 5083-H321 alloy microstructure. The onion ring patterns were clearly seen in Figs. 4c,d. Immediately adjacent to the nugget, there is the plastically deformed and heat affected so-called "thermo-mechanically affected zone (TMAZ)", which has only been affected by the heat flow [12]. The transition between the two nugget zones and thermo-mechanically affected zone are clearly visible in FS welded 5083-H321 alloy as shown in Fig. 4d. The sight of the top surface of the weld bead shows semicircular rings referred as banded microstructure.

The deformed microstructure of the base material has been replaced by equiaxed grains with little substructure. This is typical of a recrystallised microstructure and similar to that found previously in 5xxx, 6xxx and 7xxx series aluminium stir welds in accordance with the former publication by Peel et al. [10].

The hardness assessment was made on double-sided MIG, TIG and FS welded metallography specimens for both first and second pass as a function of lateral distance from the weld line for each weld at 1 mm depth of the cross-section with 200 g test load for 10 s using Future-Tech FM 700 microhardness tester. Figure 5a shows the hardness distributions of welded joints.

Figure 5b shows the average tensile properties of double-sided MIG, TIG and FS welded joints. It can be seen from the figure that the tensile properties of each joint are lower than those of the base material. Examination of the tensile test results of double-sided MIG, TIG and FS welded joints have demonstrated that the average joint efficiency values of the welded joints are 79 %, 81 % and 80 % of the base material, respectively. It has been observed that MIG and TIG welded specimens were broken from the weld metal zones. The weld metal of fusion welded non-heat treatable aluminium alloys is typically the weakest part of the joint [19]. This situation is confirmed in the hardness distribution in Fig. 5a. Heat provided by welding process is responsible of the decay of mecha-

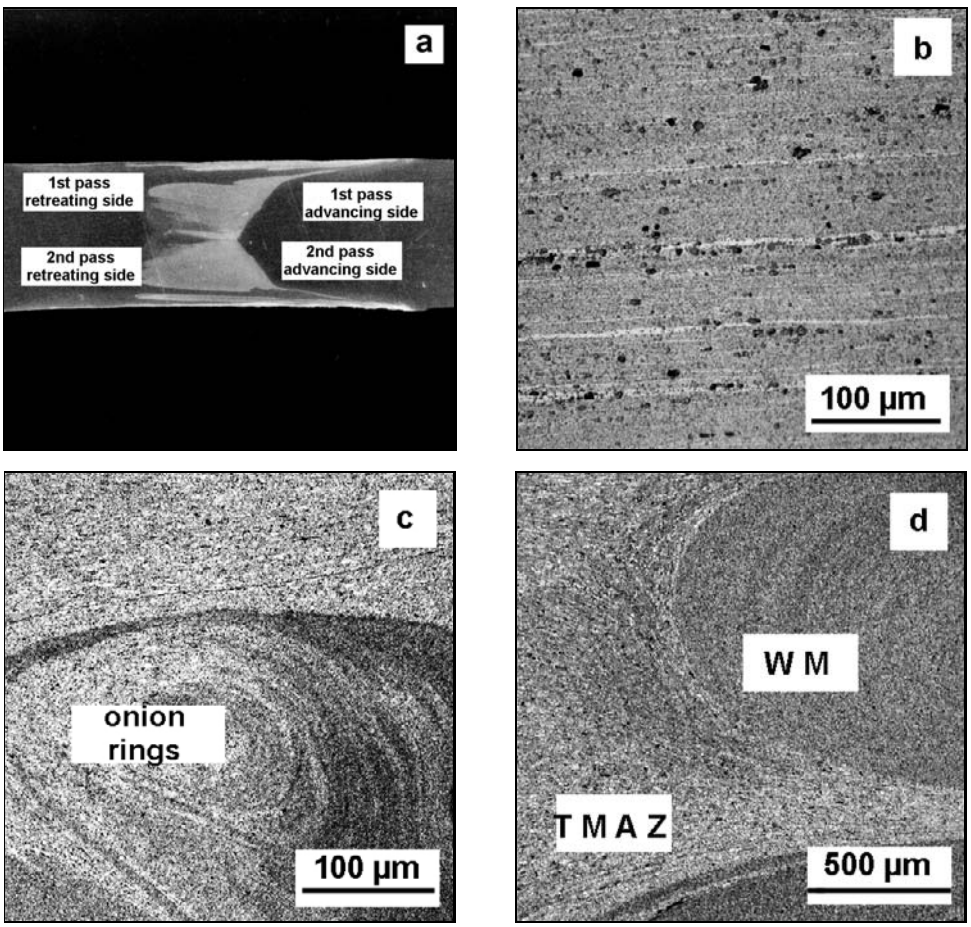

Fig. 4. Light macrostructure of FS welded 5083-H321 alloy (a) and microstructures of the alloy: BM (b), WM (c), TMAZ + WM of double passes (d).

nical properties, due to softening induced in the alloy. The strength increasing effect of strain hardened 5083--H321 aluminium alloy was eliminated by the high heat input of fusion welding and porosities in weld metal are the reasons of this situation. However, it was observed that the failure locations were in thermo--mechanically affected zones (TMAZ) from advancing side of FS welded specimens after tensile test. The weakest parts of FS welded joints were observed as TMAZ as is also confirmed in Fig. 5a with the decrease of hardness values in TMAZ. It is interesting that the hardness plots of MIG, TIG and FS welded joints were in the same order of mechanical efficiencies. The order observed was as TIG, FSW and MIG.

The 80% joint efficiency of FSW 5083-H321 specimens is a better result than the strength value proposed and discussed in an earlier publication carried out and reported by Liu et al. [13] in which the joint efficiency was determined as 73%.

The face and root bend test of the samples revealed, that although some samples of MIG and TIG welded joints contained cracking defects, no crack was detected in all face and root bend samples of FS welded joints. Figure 5c shows the bend test failure caused by under-crack defect detected in MIG welded joint, and Fig. 5d illustrates the weld metal crack of TIG welded joint. This provides one more advantage of FSW process compared to fusion welding processes.

Figures 6a–f illustrate the macrographs and SEM photographs of fracture surfaces of the tensile test specimens. Figure 6b is the enlarged SEM photograph of MIG welded sample showing a dimple pattern that indicates ductile fracture and the porosity in this matrix occurred. Figure 6d also contains the SEM photograph of dimple patterns and some microvoids, which caused fracture to initiate in TIG welded joint. Figures 6e,f exhibit the fracture phenomena of FS welded specimens. Tensile testing of these joints showed that cracking tended to occur initially at the upper region of the joint and propagated toward the bottom region. The interesting fracture occurred from onion ring fragments as layers with ductile-brittle mixed type was similar to cast alloy structure that caused to reduce the joints strength.

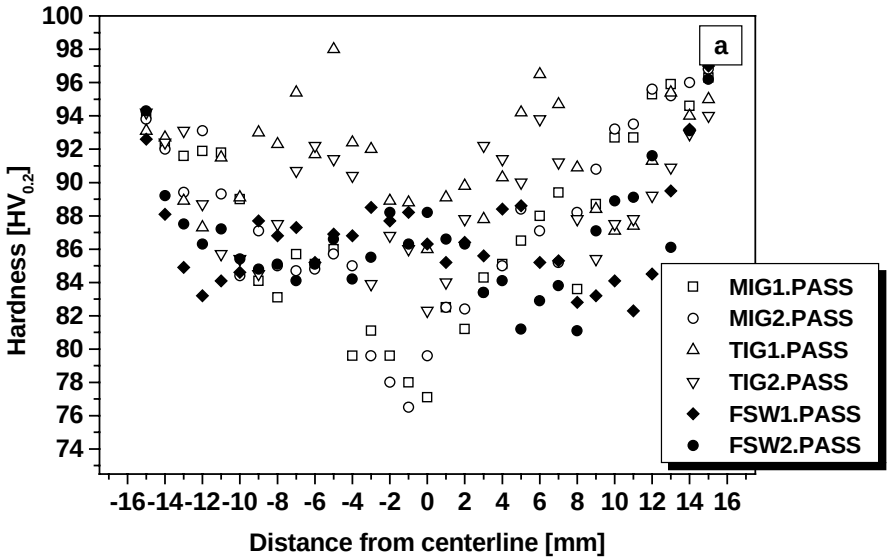

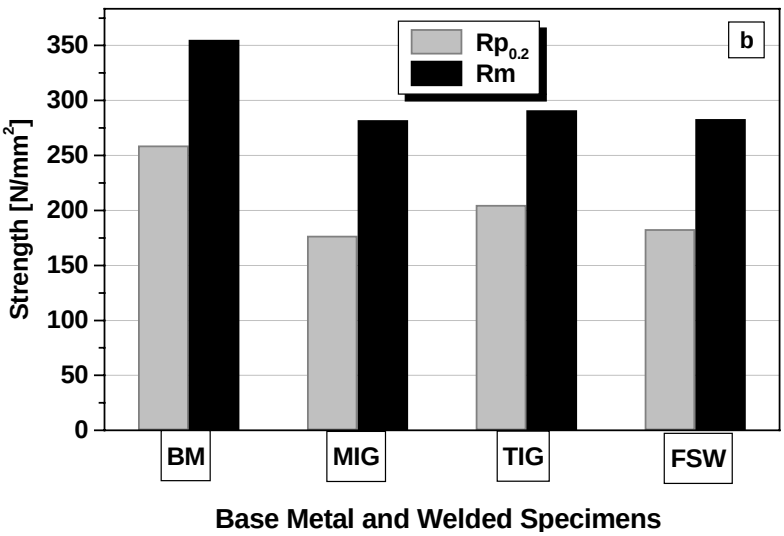

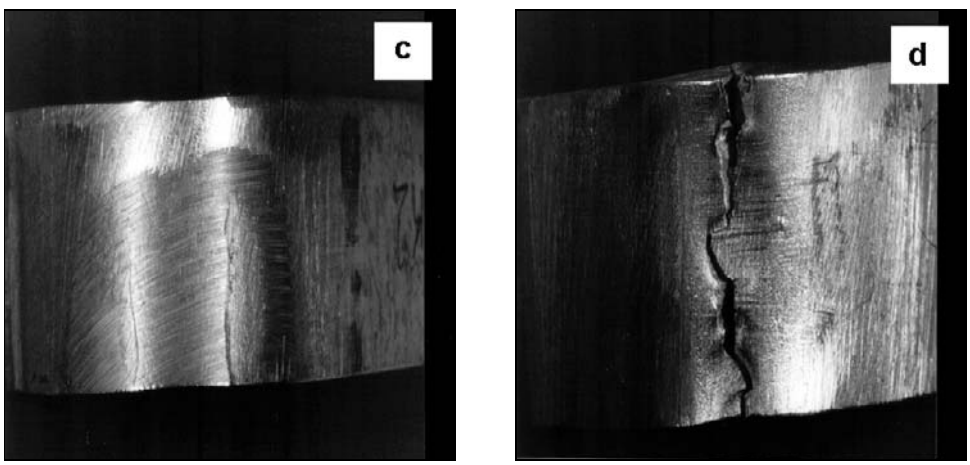

Fig. 5. First and second pass hardness distributions of MIG, TIG and FS welded joints, respectively (a), comparison of average tensile properties of the base metal with welded joints (b), the failures observed in the root and face bend test specimens of MIG (c) and TIG (d) welded joints.

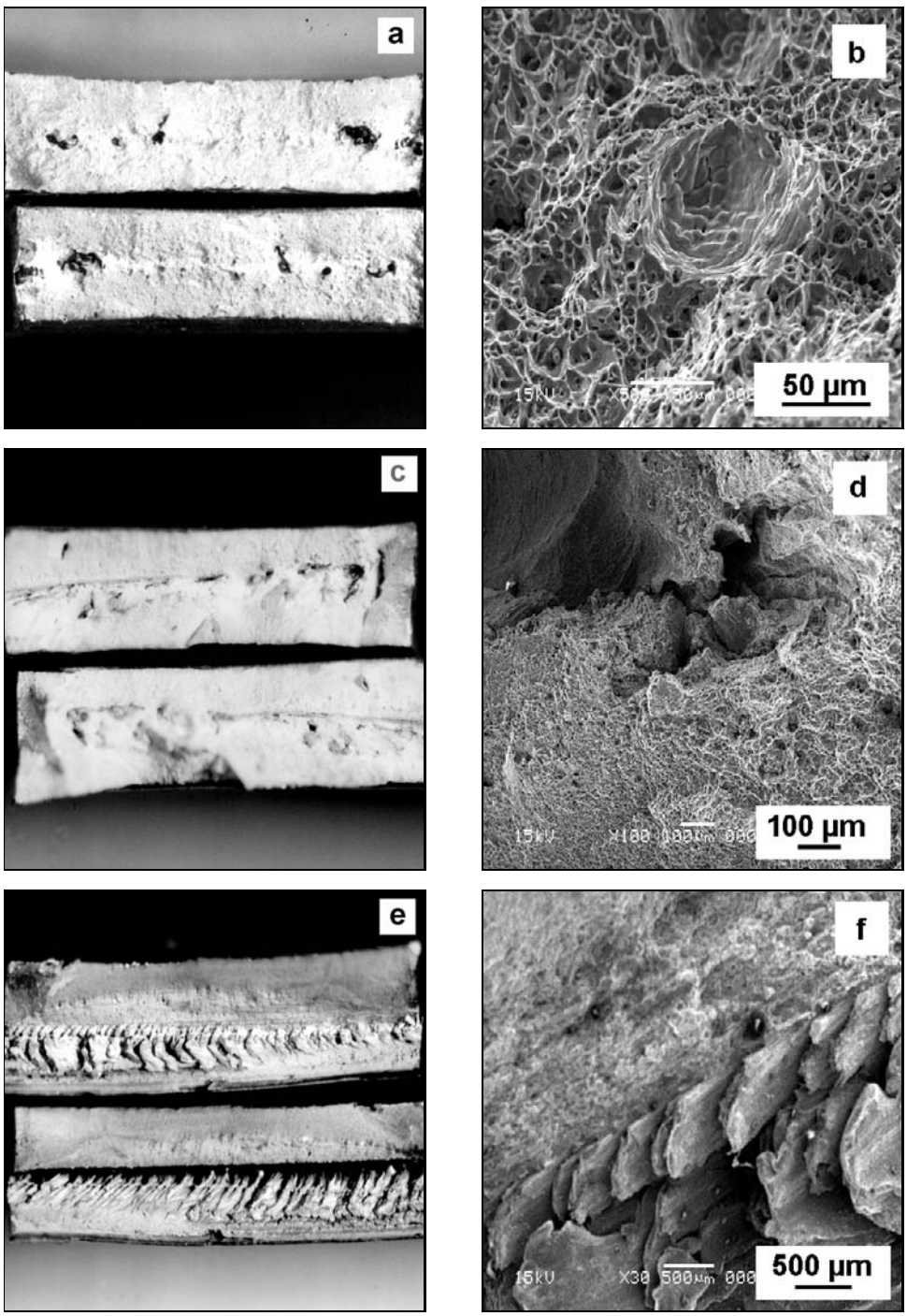

Fig. 6. Light macrographs and SEM images of the fracture surfaces of the welded specimens: light macrograph (a) and SEM photo (b) of MIG welded joint, light macrograph (c) and SEM photo (d) of TIG welded joint, light macrograph (e) and SEM photo (f) of FS welded joint.

4. Conclusions

The conventional fusion welding processes – MIG and TIG and a new solid state welding process FSW were successfully applied to the joining of 5083-H321 aluminium alloy from both sides. Microstructural properties, hardness distributions, mechanical properties and examining of fracture surfaces of double-side MIG, TIG (with X-groove) and FS (with I-groove) welded 5083-H321 alloy have been studied in the present work. Following conclusions are drawn:

(1) The microstructure of double stir zones was

mainly composed of onion ring structures in double nugget zones with fine and equiaxed grains and TMAZ were observed.

(2) The hardness of the weld zone confirmed the joint efficiencies of welded plates as observed in tensile test.

(3) The present study has demonstrated that the tensile properties of FS welded joints were satisfactory as/than TIG and MIG welded joints. Though all failure locations were detected as weld metal in fusion welding processes, all failure locations of FS welded specimens were occurred at TMAZ advancing side.

(4) Bend tests of welded plates have shown that FS welded specimens do not include any defect like fusion welded specimens.

(5) The LM and SEM examination of fracture surfaces revealed porosities in MIG and TIG welds that have caused mechanical results to decrease; however FS welds do not include any weld defects. Furthermore, ductile-brittle mixed type fracture has been occurred in FS welded joints weld zones as layers from the onion rings.

(6) No filler metal and groove preparation were needed in FSW process, the surface appearance approaches to that of a rough-machined surface. This situation reduces the production costs.

(7) The FSW process is a solid state welding process with process temperatures lower than fusion techniques, thus avoiding problems such as porosity, cracking and distortion. These are also the advantages of FSW process in comparison with fusion welding processes such as MIG and TIG.

Acknowledgements

The authors would like to thank FNSS Defence Industry Company for providing aluminium alloys investigated in present paper and for financial support of Kocaeli University Research Fund in scope of research project (Project No: 2004/51). Acknowledgements to Prof. Dr. Sadi Karagoz and his team for the SEM photographs.

References

[1] MATHERS, G.: The Welding of Aluminium and Its Alloys. Cambridge, Woodhead Publishing Limited 2002.
[2] ANDERSON, T.: Welding Journal, *81*, 2002, p. 77.
[3] ANDERSON, T.: Welding Journal, *83*, 2004, p. 28.
[4] JOHNSEN, M. R.: Welding Journal, *78*, 1999, p. 35.
[5] KALLEE, S. W.—DA VENPORT, J.—NICHOLAS, E. D.: Welding Journal, *81*, 2002, p. 47.
[6] DAWES, C. J.—THOMAS, W. M.: Welding Journal, *75*, 1996, p. 41.
[7] COLLIGAN, K. J.—KONKOL, P. J.—FISHER, J. J.—PICKENS, J. R.: Welding Journal, *82*, 2003, p. 34.
[8] THREADGILL, P.: TWI Bulletin Reprint 513/2/97. Cambridge 1997.
[9] DAWES, C. J.—THOMAS, W.: TWI Bulletin 6. Reprint 493/6/95. Cambridge 1995, p. 124.
[10] PEEL, M.—STEUWER, A.—FREUSS, M.—WITHERS, P. J.: Acta Materialia, *51*, 2003, p. 4791.
[11] JAMES, M. N.—HATTINGH, D. G.—BRADLEY, G. R.: International Journal of Fatigue, *25*, 2003, p. 1389.
[12] LARSSON, H.—KARLSSON, L.: Svetsaren, *2*, 2000, p. 6.
[13] LIU, H. J.—FUJII, H.—MAEDA, M.—NOGI, K.: Transactions of Nonferrous Metals. Society of China, *13*, 2003, p. 14.
[14] DICKERSON, T. L.—PRZYDATEK, J.: International Journal of Fatigue, *25*, 2003, p. 1399.
[15] SHIGEMATSU, I.—KWON, Y. J.—SUZUKI, K.—IMAI, T.—SAITO, N.: Journal of Materials Science Letters, *22*, 2003, p. 353.
[16] JAMES, M. N.—BRADLEY, G. R.—LOMBARD, H.—HATTINGH, G.: Fatigue Fract Eng Mater Struct., *28*, 2005, p. 245.
[17] REYNOLDS, A. P.—LOCKWOOD, W. D.—SEIDAL, T. U.: Materials Science Forum, *331–337*, 2000, p. 1719.
[18] MCLEAN, A. A.—POWELL, G. L. F.—BROWN, I. H.—LINTON, V. M.: Science and Technology of Welding and Joining, *8*, 2003, p. 462.
[19] CROSS, C. E.—KOHN, M. L.: ASM Handbook Welding, Brazing and Soldering, ASM Int., USA, Vol. 6, 2000, p. 537.
[20] STEVENS, R. H.: ASM Handbook Metallography and Microstructures. ASM Int., USA, Vol. 9, 2000, p. 362.